MOLECULAR MEDICINE REPORTS 21: 320-328, 2020

Cortex Mori Radicis extract promotes neurite outgrowth in diabetic rats by activating PI3K/AKT signaling and inhibiting Ca^{2+} influx associated with the upregulation of transient receptor potential canonical channel 1

MIN LU[1], TAO YI[2], YONG XIONG[2], QIAN WANG[3] and NINA YIN[4]

[1]Department of Histology and Embryology, School of Basic Medical Sciences, Hubei University of Medicine, Shiyan, Hubei 442000; [2]College of Acupuncture and Moxibustion; Departments of [3]Pathogen Biology and [4]Anatomy, School of Basic Medical Sciences, Hubei University of Chinese Medicine, Wuhan, Hubei 430065, P.R. China

Received April 10, 2019; Accepted October 16, 2019

DOI: 10.3892/mmr.2019.10839

Abstract. Cortex Mori Radicis extract (CMR) has various pharmacological properties, such as anti-inflammatory, anti-allergic and anti-hyperglycemic effects. However, the effects and mechanisms of CMR in the neuroregeneration of diabetic peripheral neuropathy (DPN) are unclear. In the present study, the effects of CMR on neurite outgrowth of dorsal root ganglia (DRG) neurons in diabetic rats were investigated and its underlying mechanisms were explored. SD rats were subjected to a high-fat diet with low-dose streptozotocin to induce a Type II diabetes model with peripheral neuropathy. CMR was then applied for four weeks continuously with or without injection of small interfere (si)RNA targeting the transient receptor potential canonical channel 1 (TRPC1) via the tail vein. Blood glucose levels, the number of Nissl bodies, neurite outgrowth and growth cone turning in DRG neurons were evaluated. The expression of TRPC1 protein, Ca^{2+} influx and activation of the PI3K/AKT signaling pathway were also investigated. The results of the present study showed that CMR significantly lowered blood glucose levels, reversed the loss of Nissl bodies, induced neurite outgrowth and restored the response of the growth cone of DRG neurons in diabetic rats. CMR exerted neurite outgrowth-promoting effects by increasing TRPC1 expression, reducing Ca^{2+} influx and enhancing AKT phosphorylation. siRNA targeting TRPC1 in the CMR group abrogated its anti-diabetic and neuroregenerative effects, suggesting the involvement of TRPC1 in the biological effects of CMR on DPN.

Correspondence to: Dr Nina Yin, Department of Anatomy, School of Basic Medical Sciences, Hubei University of Chinese Medicine, 1 Huangjiahu West Road, Hongshan, Wuhan, Hubei 430065, P.R. China
E-mail: yinnina-hbtcm@hotmail.com

Key words: Cortex Mori Radicis extract, diabetic peripheral neuropathy, neuroregeneration, transient receptor potential canonical channel 1, PI3K/AKT signaling

Introduction

There are an increasing number of cases of type II diabetes worldwide, including in Eastern and Western countries. Type II diabetes accounts for ~90% of all patients with diabetes and is becoming a global public health challenge (1). As a common complication of diabetes, diabetic peripheral neuropathy (DPN) is characterized by swelling, degeneration, necrosis of dorsal root ganglia (DRG) neurons accompanying axonal degeneration and atrophy, leading to a high rate of disability and mortality in patients with type II diabetic (2). Western medicines, such as methylcobalamin and neurotrophin, are usually used in clinical treatment; however, the therapeutic effects are poor in patients with DPN (3). Additionally, the high cost also increases patient burden, for example, the annual cost of DPN and its complications was 4.6-13.7 billion dollars in the US in 2001 (4). Traditional Chinese medicine, such as Chinese herbs, acupuncture and massage, is now attracting attention for the treatment of DPN due to its lower cost, accessibility and efficacy (5).

Cortex Mori Radicis extract (CMR), collected from the root bark of some Morus species, including *M. alba*, *M. mongolica*, *M. cathayana*, and *M. australis*, has been used as an anti-diabetic agent in traditional Chinese medicine for years (6). A previous study reported that hot water extracts from CMR (*Morus alba L.*) possessed hypoglycemic activity in streptozotocin (STZ)-induced diabetic mice (7). CMR was also reported to attenuate myocardial damage in diabetic rats, such as cardiac hypertrophy and fibrosis (8). Our previous study indicated that CMR induced the neurite outgrowth in pheochromocytoma PC12 cells and the primary cortical neuron of rats (9). These previous findings suggested that CMR possesses anti-diabetic and neuroprotective potential, and the roles of CMR have been demonstrated using different methods, including *in vivo* vs. *in vitro* experiments. However, few previous studies have focused on the effects of CMR on neuroregeneration of DPN in Type II diabetics and a detailed mechanism remains unclear.

Therefore, the present study was designed to investigate the effects of CMR on DPN in diabetic rats using DRG neurons and explore the underlying mechanisms. The results of the present study showed that CMR induced and promoted the neurite outgrowth of DRG in diabetic rats, which was associated with the activation of PI3K/AKT signaling and inhibition of Ca^{2+} influx by upregulating transient receptor potential canonical 1 (TRPC1).

Materials and methods

Preparation of CMR extract. CMR was purchased from Anhui Tienho Herbal Source Company. CMR (100 g) was thinly sliced with scissors soaked in 500 ml distilled water at 50˚C for 3 h, and concentrated using a rotary evaporator (BUCHI B-480; BUCHI, Ltd.) at 60 rpm and 70˚C for 2 days. The concentrated extracts were lyophilized using a freeze dryer (FDU-540; EYELA) for 24 h. After the lyophilization, a yellow-brownish active powder was obtained (yield=11.1 g).

Animals. A total of 45 Male Sprague-Dawley rats (5-6 weeks old) weighing 200±20 g were obtained from Hubei Research Center of Laboratory Animals. They were maintained at room temperature (24±2˚C) and relative humidity 45-55% under a 12-h light/dark cycle. Food and water were provided *ad libitum* throughout the experiments.

Groups. The rats were randomly divided into 5 groups (n=8 each group): i) Control group (control), fed with a standard diet, gavaged with normal saline; ii) type II diabetic model group (model), induced with high-fat diet/low-dose STZ and gavaged with normal saline; iii) CMR treatment group (CMR), diabetic model followed by gastrointestinal treatment with CMR; iv) CMR plus TRPC1-small interfering (si-)RNA treatment group (CMR+si-TRPC1), diabetic model treated with CMR and a tail vein injection of TRPC1-si-RNA; and v) CMR plus control-si-RNA treatment group (CMR+si-Control), diabetic model treated with CMR and a tail vein injection of Control-siRNA.

High-fat diet/low-dose STZ-induced diabetic model. The control group was fed with a normal diet, which contained 4.25 gm% fat. The other four groups were fed with a high-fat diet for 8 consecutive weeks (1-8 weeks), which contained 24 gm% fat, 24 gm% protein and 41 gm% carbohydrate. Following this, the high-fat-diet rats were treated with STZ (30 mg/kg in 0.9% NaCl, i.p.; Sigma-Aldrich) in weeks 5-8 (once per week; a total of 4 times). Diabetes was verified by evaluating the fasting blood glucose levels using glucose oxidase reagent strips (Aviva Accu-Chek; Roche Diagnostics GmbH), a glucose level >13.9 mM was considered to indicate diabetes (10).

Treatment with CMR and injection via tail vein delivery of siRNA. Diabetic rats were subjected to 100 mg/kg CMR (lot no. 14015121; Beijing Tcmages Pharmaceutical Co., Ltd.) via gastrointestinal treatment for 4 consecutive weeks (once a day in weeks 9-12) in CMR group (11). Another two groups of diabetic rats were treated with 100 mg/kg CMR together with the tail vein delivery of TRPC1-si-RNA (0.1 mg/kg; 5'-GAA CAUAAAUUGCGUAGAU-3'; OriGene Technologies, Inc.) or Control-si-RNA (0.1 mg/kg; 5'-UAGCGACUAAACACAUCA A-3'; OriGene Technologies, Inc.) in 2 ml PBS via rapid tail vein delivery (5-10 sec), once every 4 days during weeks 9-12 (a total of 6 times), as shown in Fig. 1A (12,13). During the experiments, the following data was collected about rats in the different groups: Weight, food intake, drink and excrement.

Nociceptive behavioral tests. Thermal nociceptive threshold was assessed by measuring the withdrawal latency on hot plate as previous described (14). The temperature of the hot-plate was maintained at 50˚C. The withdrawal latency started from putting the mouse on the plate and terminated when a brisk withdrawal or paw flinching was observed. A cut-off time of 30 sec was set to avoid lesions on the paw. The mechanical nociceptive threshold was quantified using the Randall-Selitto paw withdrawal test (15) using an analgesy meter (Ugo Basile S.R.L.) that generates a linearly increasing mechanical force. Results represents the maximal pressure (g) tolerated by the animal. The test was repeated three times with each rat, and the mean value was calculated for evaluation.

Hematoxylin and eosin (H&E) staining for the evaluation of Nissl bodies. The rats were deeply anesthetized using sodium pentobarbital (50 mg/kg, i.p.) and no contraction response was observed when rat paws were clamped with tweezers. Subsequently, rats were transcardially perfused with 100 ml ice-cold PBS (pH 7.4) followed by 500 ml 4% paraformaldehyde. After perfusion, the spine was surgically isolated followed by a longitudinal incision, the spinal cord was carefully removed and the intervertebral foramen was exposed. DRGs (T8-L5) were isolated and obtained. DRGs were post-fixed in the same fixatives for 90 min at room temperature and cryoprotected overnight at 4˚C in PBS containing 30% sucrose. The DRGs were embedded in optimal cutting temperature compound (Bayer Corporation), frozen and then cut into 15 μm sections. The sections were mounted on gelatin coated slides for H&E staining to observe changes in Nissl bodies. According to the manufacturers' protocol (C0105, Beyotime Institute of Biotechnology), the slides were stained in hematoxylin for 5 min and washed with H_2O for 10 min at room temperature. After dipping in 80% EtOH, the slides were stained with Eosin for 30 sec, and dipped sequentially in 95% EtOH and 100% EtOH. Then, the slides were immersed in xylene for 5 min, and images were captured using a Nikon Eclipse Ti-S microscope (Nikon Corporation) at 400x magnification. All sections were randomized and evaluated by two trained observers who were blinded to the treatment groups.

DRG neuron culture. After deep anesthesia induced by intraperitoneal injection of sodium pentobarbital (50 mg/kg), rats were unconsciousness with a slow respiratory and heart rate. DRGs (T8-L5) were isolated following the aforementioned protocol without intracardiac perfusion. The DRGs were digested with 0.5% trypsin and 1% collagenase (type IA; Invitrogen; Thermo Fisher Scientific, Inc.) at 37˚C for 1 h to obtain a single cell suspension. Following this, 10% FBS (Invitrogen; Thermo Fisher Scientific, Inc.) was added to

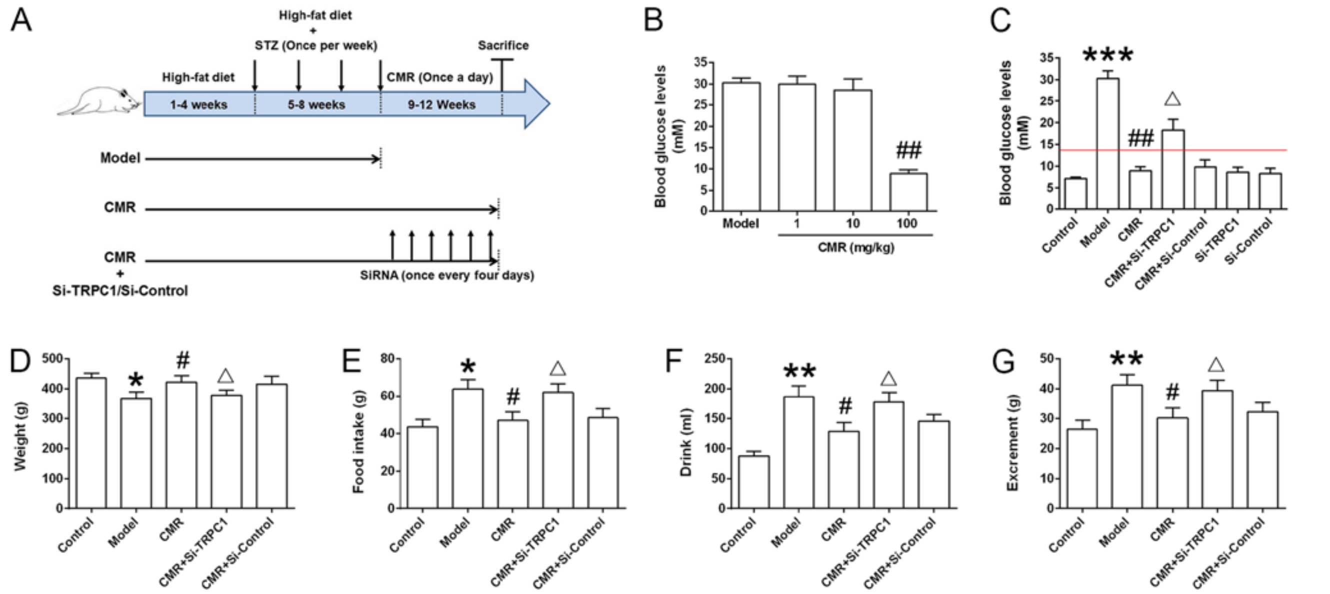

Figure 1. Effect of CMR treatment on the blood glucose levels of diabetic rats. (A) Schematic diagram of the experimental procedure. Rats were fed a high-fat diet for 8 weeks. During weeks 5-8, STZ (30 mg/kg) was injected intraperitoneally once a week. The rats were then subjected to 4 continuous weeks of CMR (once a day) with or without the tail vein delivery of si-TRPC1 of si-control (once every 4 days). The rats were sacrificed and the samples were collected 24 h after the last CMR treatment. (B) The blood glucose levels between the diabetic model and CMR treatment groups, including low (1 mg/kg), moderate (10 mg/kg) and high (100 mg/kg) doses of CMR, were measured through the tail vein using a blood glucose meter. (C) At the end of the experiment, the blood glucose levels of rats from the different groups were measured and statistically analyzed. The red line indicates a blood glucose level of 13.9 mM. (D) Weight, (E) food intake, (F) drinking water and (G) excrement were monitored. The parameters refer to the average value per rat in the different groups (n=5 per group). *P<0.05, **P<0.01, ***P<0.001 vs. control; #P<0.05 and ##P<0.01 vs. model; ΔP<0.05 vs. CMR. STZ, streptozotocin; CMR, Cortex Mori Radicis extract; TRPC1, transient receptor potential canonical channel 1; si-, small interfering RNA.

stop digestion and the cells were centrifuged for 10 min at 1,000 rpm. The cells were resuspended and cultured in the neurobasal medium (Invitrogen; Thermo Fisher Scientific, Inc.) supplemented with 0.5 mM glutamine, 100 U/ml penicillin and 100 μg/ml streptomycin (Gibco; Thermo Fisher Scientific, Inc.) at 37˚C in a 5% CO_2 incubator.

Assessment of total neurite outgrowth. DRG neurons from different groups were loaded with fura-2/AM (2 μM; S1052, Beyotime Institute of Biotechnology) at room temperature for 30 min to assay neurite outgrowth as previously described (16). The cells were cultured on round coverslips, and then treated with fura-2/AM. Images were captured using a Leica DMI 6000B fluorescence microscope (Leica Microsystems GmbH) controlled using SlideBook software 4.2 (Intelligent Imaging Innovations, Inc). The length of neurite outgrowth was assessed by measuring the total length from the cell body to the end of all neuritis. The final length was the sum of all neurites that were measured from one cell body.

Growth cone turning assay. To assess growth cone turning, a micropipette was placed 15 mm away from the growth cone center at an angle of 45˚ with respect to the initial direction of the neurite extension. Axons were positioned with their growth cones 100 μm away from a glass micropipette containing nerve growth factor (NGF, 50 ng/ml) with their direction of growth at 45˚ to the pipette tip. NGF was expelled at 2 Hz using 3 psi to create gradients with a 10-15% change in concentration across 10 μm. Phase contrast images were acquired at a magnification of x20 for 1 h at 1 min intervals with a Zeiss Axio Observer (Zeiss GmbH) at room temperature.

Reverse transcription-quantitative (RT-q)PCR. Neurons were collected and total RNA was extracted using TRIzol reagent (Invitrogen; Thermo Fisher Scientific, Inc.). RT was performed using a Reverse Transcription kit (Takara Biotechnology Co., Ltd.). The reaction conditions were as follows: 37˚C for 15 min, 85˚C for 5 sec and a 4˚C hold. The expression levels of TRPC1 were determined using qPCR with the Real-Time PCR System 7500 Fast (Applied Biosystems; Thermo Fisher Scientific, Inc.). The following primers were synthesized by Sangon Biotech Co., Ltd.: TRPC1 forward, 5'-GCAGAACAGCTTGAAGGAGTG-3' and reverse, 5'-CACTAGGCAGCACATCACCT-3'; and GAPDH forward, 5'-TCTCTGCTCCTCCCTGTTCTA-3' and reverse, 5'-GCCAAATCCGTTCACACCG-3'. The amplification conditions were as follows: 50˚C for 2 min and 95˚C for 10 min, followed by 40 cycles of 95˚C for 15 sec, 60˚C for 30 sec and 72˚C for 30 sec. The fold change in mRNA expression was quantified using the $2^{-\Delta\Delta Cq}$ method (17) and GAPDH was used for normalization.

Western blotting. Neurons were collected and lysed with RIPA buffer (Beyotime Institute of Biotechnology) and the protein concentration was determined using a BCA Protein Assay kit (Pierce; Thermo Fisher Scientific, Inc.). Proteins (25 μg) were resolved using 10% SDS-PAGE, transferred to PVDF membranes and probed with antibodies against TRPC1 (cat. no. sc-133076; Santa Cruz Biotechnology, Inc.), PI3K (p110α, 1:1,000; cat. no. 4255; Cell Signaling Technology, Inc.), AKT (1:1,000, cat. no. 4691; Cell Signaling Technology, Inc.), phospho-Ser473 AKT (1:2,000, p-AKT; cat. no. 4060; Cell Signaling Technology, Inc.) and GAPDH (1:1,000, cat. no. 5174; Cell Signaling Technology, Inc.). The membranes were then incubated with horseradish peroxidase-conjugated secondary antibody [horse anti-mouse IgG (1:2,000, cat. no. 7076) or goat anti-rabbit IgG (1:2,000, cat. no. 7074)] at room temperature for 1 h. Immunoreactive bands were visualized using ECL (SignalFire™ Plus ECL Reagent, cat. no. 12630, Cell Signaling Technology, Inc.) and bands were scanned using a scanner (HP Scanjet 7400C; Hewlett Packard). Optical density for each band was assessed using ImageJ analysis software (version 1.60, National Institutes of Health). Sample loading was normalized by quantities of GAPDH detected in parallel.

Calcium imaging. Ratiometric imaging of intracellular Ca^{2+} using cells loaded with Fura-2/AM. DRG neurons were seeded in a 6-well plate ($5x10^5$ cells/well) and were cultured for 24 h. Coverslips with cells were placed in a cation-safe solution composed of (107 mM NaCl, 7.2 mM KCl, 1.2 mM $MgCl_2$, 11.5 mM glucose, 20 mM HEPES-NaOH, pH 7.3) and loaded with Fura-2/AM (2 μM final concentration) for 30 min at 37˚C. Cells were washed and Ca^{2+} measurements were performed using a Leica DMI 6000B fluorescence microscope controlled using SlideBook software. Intracellular Ca^{2+} measurements are shown as the 340/380 nm ratio obtained from groups of single cell (~50 cells).

Statistical analysis. Data are presented as the mean ± SD from at least 3 independent experiments. Comparisons between two groups were conducted using a one-way ANOVA and Bonferroni-Dunn test for multiple comparisons using Prism 5.0 software (GraphPad Software, Inc.). P<0.05 was considered to indicate a statistically significant difference.

Results

CMR treatment reduces the blood glucose levels of diabetic rats. As shown in Fig. 1B, a high dose of CMR (100 mg/kg) decreased the blood glucose levels of diabetic rats. Compared with the model group, the blood glucose levels in diabetic rats following CMR treatment were significantly decreased (30.3±1.96 vs. 8.92±1.02 mM in the model and CMR groups, respectively; P<0.01; Fig. 1C). Additionally, CMR treatment restored the weight of diabetic rats and showed an inhibitive effect on food intake, drink and excrement in rats who received an injection of STZ (Fig. 1D-G). siRNA-TRPC1 treatment abrogated the suppressive effect of CMR in diabetic rats (8.92±1.02 vs 18.3±2.14 mM in the CMR vs. CMR + si-TRPC1; P<0.05), suggesting that TRPC1 is involved in the anti-diabetic effects of CMR (Fig. 1C-G).

CMR improved nerve functions in rats with STZ-induced DPN. To evaluate the effects of CMR on nerve functions in rats with DPN, thermal hypoalgesia and the mechanical threshold was assessed. CMR significantly inhibited the increase of thermal latency (Fig. 2A). Compared with the model group, CMR prevented a decrease in the mechanical threshold (Fig. 2B). Consistent with the aforementioned results, si-TRPC1 treatment reversed the protective effects of CMR on nerve functions in diabetic rats.

CMR reverses the loss of Nissl bodies in the DRG neurons of diabetic rats. Pathological changes in the DRG neurons

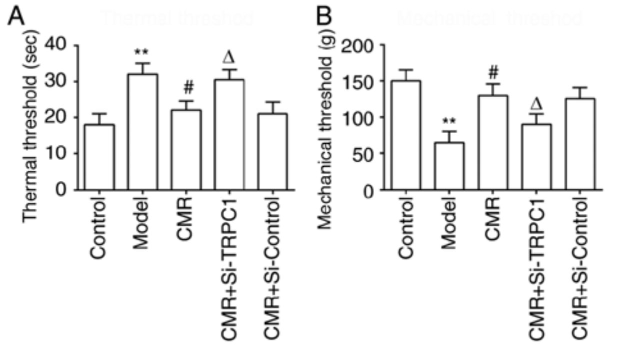

Figure 2. Effects of CMR on thermal hypoalgesia and the mechanical threshold in diabetic rats. (A) The paw withdrawal latency of rats from the different groups was assessed using a hot-plate. (B) The mechanical threshold of rats in the different groups was assessed. **P<0.01 vs. control; #P<0.05 vs. model; ΔP<0.05 vs. CMR. CMR, Cortex Mori Radicis extract; TRPC1, transient receptor potential canonical channel 1; si-, small interfering RNA.

were investigated by assessing the morphology of Nissl bodies using H&E staining. As shown in Fig. 3, DRG neurons in diabetic rats showed a loss of Nissl bodies. However, Nissl body dissolution was distinctly decreased with CMR treatment. Compared with the CMR group without TRPC1-siRNA treatment, Nissl bodies showed more pathological changes following si-TRPC1 transfection.

CMR induces the neurite outgrowth of DRG neurons in diabetic rats. To analyze neurite outgrowth, the total lengths of neurites were measured. Compared with the control group, the total neurite outgrowth in the DRG neurons of diabetic rats were significantly decreased (119.8±3.7 vs. 43.4±5.86 μm in the control and model groups, respectively; P<0.01; Fig. 4). Conversely, CMR treatment induced the neurite outgrowth of DRG neurons (43.4±5.86 vs. 111.2±6.76 μm in the model and CMR groups, respectively; P<0.01). si-TRPC1 transfection reduced the effect of CMR on the neurite outgrowth of DRG neurons in diabetic rats (111.2±6.76 vs. 57.0±6.5 μm in the CMR and CMR + si-TRPC1groups, respectively; P<0.05; Fig. 4).

CMR restores the response of the growth cone to NGF in diabetic rats. The chemotropic responses of DRG neurons as assessed by exposing growth cones to gradients of NGF. The growth cones in the model group exhibited no apparent bias in the direction of extension. CMR treatment evoked a marked chemotropic turning response toward the source of the NGF. Transfection with si-TRPC1 in the CMR group showed little effect on growth cone turning in response to NGF (Fig. 5).

CMR upregulates TRPC1 and inhibits Ca^{2+} influx in the DRG neurons of diabetic rats. As shown in Fig. 6A, TRPC1 was successfully knocked down in si-TRPC1 rats. CMR treatment upregulated the expression of TRPC1 compared with the model group at the mRNA and protein levels (Fig. 6B-D). si-TRPC1 transfection suppressed the increase in the expression level of TRPC1 expression at protein level following CMR administration. Additionally, the Ca^{2+} influx in the DRG neurons from diabetic rats was significantly increased compared with the control group. CMR treatment inhibited

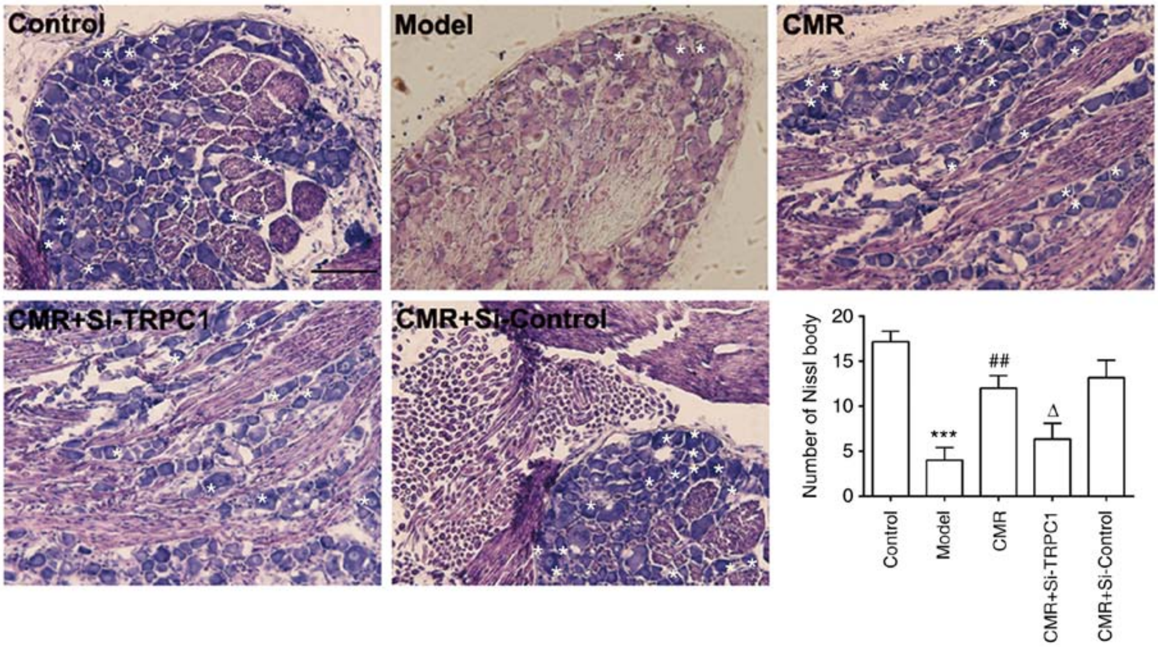

Figure 3. Effect of CMR on Nissl bodies in DRG neurons in diabetic rats. DRG neurons were separated and extracted from the spinal cord and fixed with 4% paraformaldehyde for frozen sectioning. Morphological changes of DRG neurons were observed, including Nissl bodies and the size of neurons. White asterisks indicate Nissl bodies. Scale bar, 50 μm. ***P<0.001 vs. control; $^{\#\#}$P<0.01 vs. model; $^{\Delta}$P<0.05 vs. CMR. CMR, Cortex Mori Radicis extract; TRPC1, transient receptor potential canonical channel 1; si-, small interfering RNA; DRG, dorsal root ganglia.

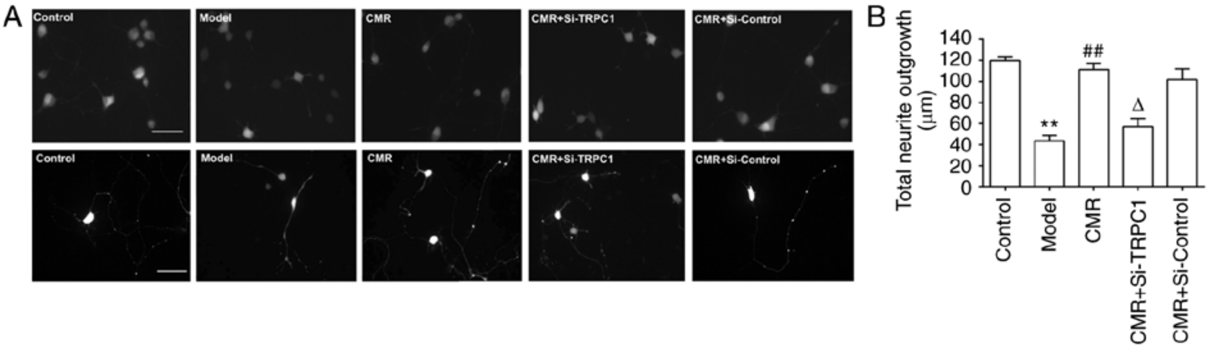

Figure 4. Effect of CMR on the neurite outgrowth of DRG neurons in diabetic rats. (A) DRG neurons were obtained and loaded with Fura-2. Morphological changes in the DRG neurons were observed, such as multicellular neurite outgrowth (top panel) and single cell neurite outgrowth (bottom panel). (B) The lengths of neurite outgrowth were measured and statistically analyzed. Scale bar, 20 μm. **P<0.01 vs. control; $^{\#\#}$P<0.01 vs. model; $^{\Delta}$P<0.05 vs. CMR. CMR, Cortex Mori Radicis extract; TRPC1, transient receptor potential canonical channel 1; si-, small interfering RNA; DRG, dorsal root ganglia.

extracellular Ca^{2+} influx in the DRG neurons of diabetic rats. Moreover, the suppressive effect of CMR on Ca^{2+} influx was partially reversed by si-TRPC1 transfection (Fig. 6E and F).

Activation of PI3K/AKT signaling participates in the neurite outgrowth-inducing effects of CMR in diabetic rats. To investigate the possible molecular mechanisms of CMR-induced neurite outgrowth in diabetic rats, the effect of CMR on the activation of PI3K/AKT signaling was assessed. As shown in Fig. 7, CMR treatment increased the expression of PI3K and enhanced the phosphorylation of AKT. On the contrary, si-TRPC1 transfection in the CMR group reduced the activation of the PI3K/AKT signaling associated with CMR treatment, suggesting that the PI3K/AKT signaling pathway may be involved in the neurite outgrowth-promoting effects of CMR in DPN.

Discussion

STZ-induced diabetic rats are one of the most frequently used animal models to study diabetes. A combination of a high-fat diet and a low dose of STZ can be used to induce a DPN model in Sprague-Dawley rats and C57Bl/6J mice (18,19). Based on the achievable treatment strategies, such as controlling hyperglycemia, encouraging neurite elongation, increasing the supply of angiogenic and neurotrophic factors, previous studies have indicated that traditional Chinese medicine can be considered and used as a promising treatment for DPN (20-23). Jiaweibugan decoction was reported to significantly ameliorate motor nerve conduction velocity in diabetic rats and to play a protective role in peripheral nerve injury (24). Bogijetong decoction had the potential to induce neurite outgrowth of DRG neurons in STZ-diabetic animals (25). Consistent with

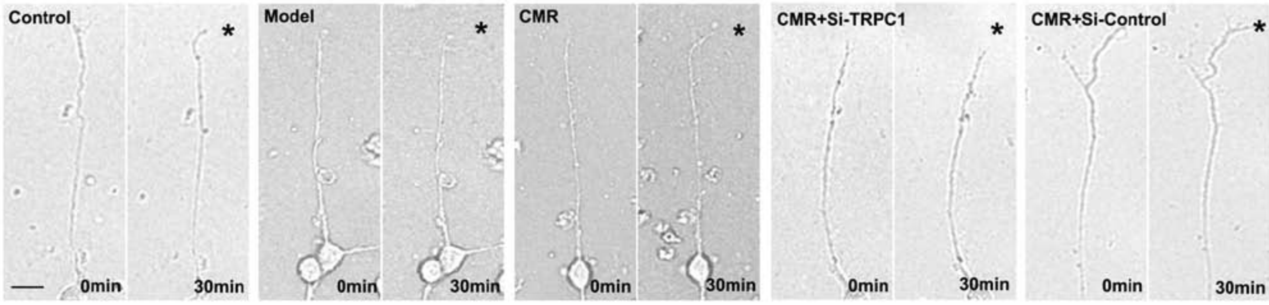

Figure 5. Effect of CMR on the growth cone of DRG cells in response to NGF. Images of growth cone in cultured DRG cells before and after 30 min exposure to NGF are shown. Asterisks indicate the NGF gradient. Scale bar, 50 μm. NGF, nerve growth factor; CMR, Cortex Mori Radicis extract; TRPC1, transient receptor potential canonical channel 1; si-, small interfering RNA; DRG, dorsal root ganglia.

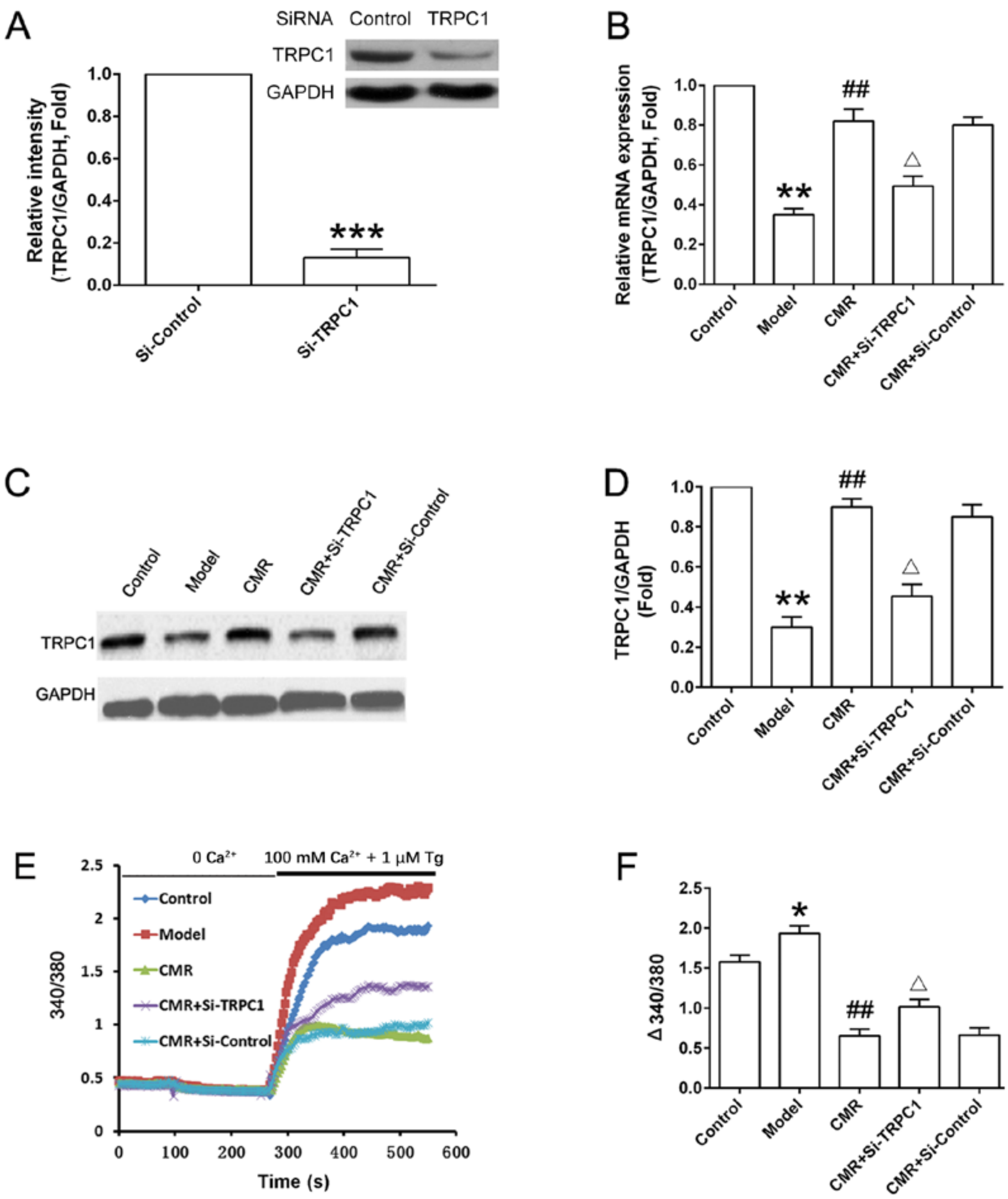

Figure 6. Effect of CMR on the TRPC1/Ca^{2+} axis in the DRG neurons of diabetic rats. DRG neurons were seeded in a 6-well plate (5x10^5 cells/well) and were cultured for 24 h. (A) Normal rats were treated with control siRNA and TRPC1 siRNA. DRG neurons were collected and TRPC1 expression was detected by western blotting and was statistically analyzed. (B) mRNA expression levels of TRPC1 in the DRG neurons from different groups were detected by reverse transcription-quantitative PCR and analyzed. (C) Protein expression levels of TRPC1 in the DRG neurons from different groups were detected by western blotting and (D) were statistically analyzed. GAPDH was used to confirm equal sample loading. (E) DRG neurons were seeded in a 6-well plate (5x10^5 cells/well) and were cultured for 24 h. Cytosolic Ca^{2+} was measured in Fura-2-loaded DRG neurons and (F) statistically analyzed (340/380). Representative traces of intracellular Ca^{2+} in DRG neurons are shown. *P<0.05, **P<0.01, ***P<0.001 vs. control; $^{##}$P<0.01 vs. model; $^{\Delta}$P<0.05 vs. CMR. CMR, Cortex Mori Radicis extract; TRPC1, transient receptor potential canonical channel 1; si-, small interfering RNA; DRG, dorsal root ganglia; Tg, thapsigargin.

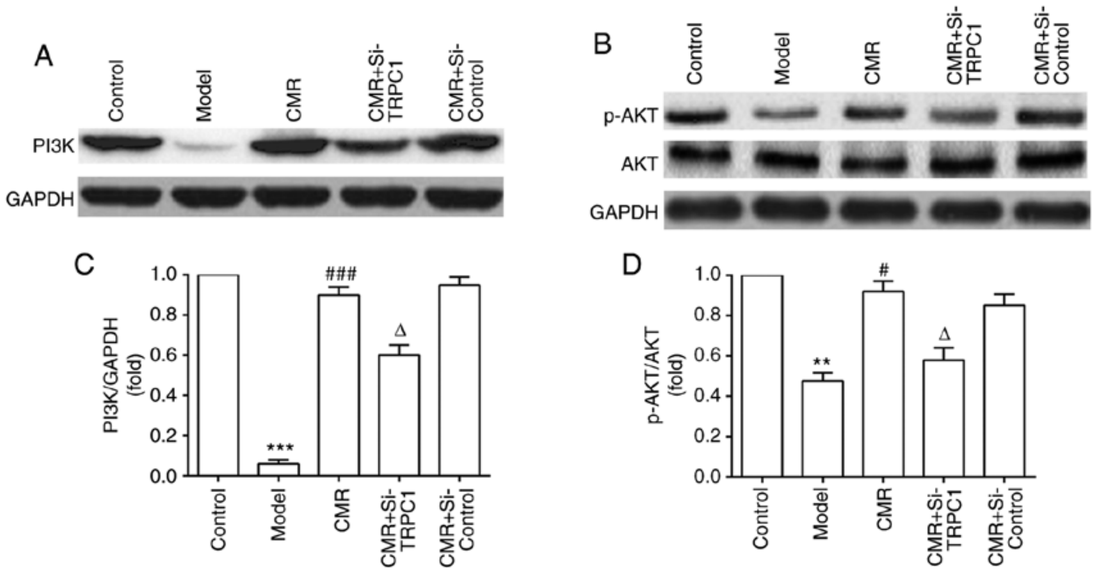

Figure 7. Effect of CMR on PI3K/AKT signaling in the DRG neurons of diabetic rats. DRG neurons were separated and the lysates were analyzed using western blotting. (A) Expression of PI3K, (B) AKT and p-AKT proteins was detected by western blotting. (C) Relative expression of PI3K (PI3K/GAPDH) was statistically analyzed. (D) Relative expression of p-AKT (p-AKT/AKT) was statistically analyzed. GAPDH was used to confirm equal sample loading. **P<0.01, ***P<0.001 vs. control; #P<0.05, ###P<0.001 vs. model; ΔP<0.05 vs. CMR. CMR, Cortex Mori Radicis extract; TRPC1, transient receptor potential canonical channel 1; si-, small interfering RNA; DRG, dorsal root ganglia; P-, phosphorylated.

these previous findings, in the present study CMR was found to lower the blood glucose levels of diabetic rats, improve nerve functions, reverse the loss of Nissl bodies, induce neurite outgrowth in DRG neurons and restore the response of growth cones to NGF, suggesting the potential of CMR on neuroregeneration in diabetic rats.

Neurite outgrowth is a critical step during neuronal differentiation and regeneration (26). Ca^{2+} has been shown to participate in the process of neurite outgrowth (27). In diabetes, neurons experience metabolic stress and mitochondrial dysfunction, which results in the deregulation of Ca^{2+} homeostasis (28). In turn, Ca^{2+} homeostasis disequilibrium aggravated the pathological cellular reactions contributing to development of diabetic neuropathies (29). Diabetic neuropathy potentiated the activity of T-type and high voltage-activated Ca^{2+} channels in primary sensory neurons (30). A recent study showed that mesenchymal stem cells improved DPN by ameliorating intracellular Ca^{2+} homeostasis (31). Ca^{2+} signaling-associated factors in DRG neurons include several types of Ca^{2+}-permeable membrane channels (32). In the brain, Ca^{2+} influx is related to the opening of TRPC1, and is frequently associated with the regulation of adult neural progenitor cells (33). Including the change of extracellular calcium influx, a previous study reported that resting intracellular Ca^{2+} rose progressively in the neurons (DRG and dorsal horn) with the duration of diabetes and that calcium mobilization from the endoplasmic reticulum decreased during diabetes (34), suggesting the involvement of calcium in the intracellular calcium pool. In the present study, Ca^{2+} influx was reduced in the CMR group compared with the diabetic model group, which suggested that Ca^{2+} influx was related to the biological activation of CMR in diabetic rats. More studies are required to investigate whether calcium in intracellular calcium pools participates in the progress of DPN.

siRNA delivery via tail vein injection in rats has been reported to have a prolonged, but not permanent, effect on target mRNA and the potential inflammatory sequelae (13). However, this technique can also be used to introduce siRNAs into the tissues of the whole animal through a rapid and large volume tail-vein injection by increasing its hydrostatic pressure (35). A previous study reported that *in vivo* tail vein delivery of siRNA to block caspase-8 or Fas could attenuate the onset of morbidity and mortality in polymicrobial sepsis (13). Similarly, this strategy was used in the present study to deliver si-TRPC1 into rats (2 ml was injected into the tail vein within 10 sec a total of six times) to knockdown TRPC1 in DRG neurons. As expected, si-TRPC1 treatment induced a decrease in TRPC1 expression at the mRNA and protein levels, which confirmed the effectiveness of siRNA

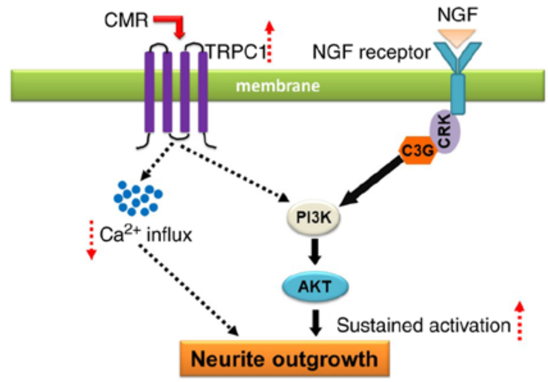

Figure 8. Schematic diagram of proposed mechanism for the neuroregenerative effect of CMR in diabetic rats. CMR treatment increases the expression of TRPC1. As a result, Ca^{2+} influx is decreased. The upregulation of TRPC1 enhanced PI3K activation and AKT phosphorylation, promoting neurite outgrowth of dorsal root ganglia neurons in diabetic rats indicating a potential new biological effect of CMR in enhancing neurite outgrowth and suggesting its potential as an alternative drug for the treatment of diabetic peripheral neuropathy in patients with type II diabetes. NGF, nerve growth factor; CMR, Cortex Mori Radicis extract; TRPC1, transient receptor potential canonical channel 1.

delivery via tail vein injection. It was notable that si-TRPC1 treatment had no obvious effect on the blood glucose in diabetic rats but showed the antagonistic effect during CMR application. The result suggested that TRPC1 only involved in the hypoglycemic effect of CMR but not fundamentally contributed to the development of diabetes although reduction in STZ-treated rats.

TRPCs belong to a superfamily of Ca^{2+}-permeable receptor-operated channels that have been reported to participate in axon regeneration of peripheral nerves (36). TRPC1 is closely related to neuron viability and growth cone sensitivity (37,38). TRPC1 promoted neurite outgrowth in PC12 cells, while TRPC5 had a suppressive effect on neurite outgrowth (39). Although TRPC1 expression was reduced in patients with diabetes and diabetic db/db mice (40), TRPC1 played an important role in the regulation of adiposity associated with type II diabetes, which functioned as a Ca^{2+} entry channel and were activated upon depletion of intracellular Ca^{2+} stores (41). Based on these previous studies, it was speculated that the regulation of TRPC1 and Ca^{2+} may participate in the neurite outgrowth in diabetic nephropathy. Consistent with this hypothesis, CMR upregulated TRPC1 expression, which was accompanied by reduced Ca^{2+} influx in the DRG neurons of rats with DPN, and the anti-diabetic and neuroprotective effects were reversed by the depletion of TRPC1.

The PI3K/AKT pathway is an important intracellular signaling pathway in regulating cellular proliferation (42). PI3K activation leads to the phosphorylation and activation of AKT, leading to downstream reactions involved in nerve regeneration in diabetic rats (43). A previous study reported that plasmacytoma variant translocation 1 regulated the occurrence and progression of DPN by activating the PI3K/AKT pathway (44). Proanthocyanidin B2 attenuated the high-glucose-induced neurotoxicity of DRG neurons through the PI3K/AKT signaling pathway (45). These previous studies suggested that there may be a link between diabetic enteric neuropathy and PI3K/AKT signaling. In the present study, CMR activated PI3K and increased the phosphorylation of AKT, resulting in the neurite outgrowth of DRG neurons. Further studies are required to determine if other signaling cascade responses participate in the biological effect of CMR in DPN, such as the p38 mitogen-activated protein kinase signaling pathway, the ERK1/2 signaling pathway, the nuclear factor-κB signaling pathway or the nuclear factor erythroid-2 related factor/heme oxygenase-1 signaling pathway.

Limitations of the present study should also be mentioned. Firstly, si-TRPC1 cannot completely mimic DPN conditions *in vivo*. A diabetic model with a TRPC1 knockout would mimic the *in vivo* scenario more closely and provide further support to the conclusions reached in the present study. Furthermore, the relationship between Ca^{2+} influx, the increase in TRPC1 expression and the activation of PI3K/AKT signaling remains unclear. Therefore, future studies should be conducted using inhibitors of Ca^{2+} influx and the PI3K/AKT pathway to further confirm the efficacy of CMR on neurite outgrowth and neural regeneration in DRG neurons in diabetic rats.

In conclusion, CMR treatment increased the expression of TRPC1, resulting in the reduced Ca^{2+} influx. The upregulation of TRPC1 was associated with the activation of PI3K/AKT signaling, which contributed, a least partially, to the neurite outgrowth-prompting effects of CMR in diabetic rats (Fig. 8). The findings of the present study provided a theoretical basis and indicated a potential use for CMR in the clinical treatment of nerve injury linked to diabetic neuropathy.

Acknowledgements

The authors would like to thank Dr Zhigang Wang (Department of Pathogen Biology, School of Basic Medical Sciences, Hubei University of Chinese Medicine, Wuhan, China) for providing advice on the experimental design and critical comments on the present manuscript.

Funding

The present study was supported by the National Natural Science Foundation for Young Scientists of China (grant no. 81600651) and the Natural Science Foundation of Hubei Province, China (grant no. 2018CFB728).

Availability of data and materials

The datasets used and/or analyzed during the current study are available from the corresponding author on reasonable request.

Authors' contributions

ML and NY designed the study, performed the experiments, analyzed the data and wrote the manuscript. TY and YX contributed to feeding and handling of mice. QW helped with the detection of calcium imaging.

Ethics approval and consent to participate

The study was approved by the Animal Care and Use Committee of Hubei University of Chinese Medicine (approval no. SYXK2012-0068).

Patient consent for publication

Not applicable.

Competing interests

The authors declare that they have no competing interests.

References

1. Xiang Y, Zhou Z, Deng C and Leslie RD: Latent autoimmune diabetes in adults in Asians: Similarities and differences between east and west. J Diabetes 5: 118-126, 2013.
2. Becker M, Benromano T, Shahar A, Nevo Z and Pick CG: Changes in the basal membrane of dorsal root ganglia schwann cells explain the biphasic pattern of the peripheral neuropathy in streptozotocin-induced diabetic rats. J Mol Neurosci 54: 704-713, 2014.
3. Xu Q, Pan J, Yu J, Liu X, Liu L, Zuo X, Wu P, Deng H, Zhang J and Ji A: Meta-analysis of methylcobalamin alone and in combination with lipoic acid in patients with diabetic peripheral neuropathy. Diabetes Res Clin Pract 101: 99-105, 2013.
4. Gordois A, Scuffham P, Shearer A, Oglesby A and Tobian JA: The health care costs of diabetic peripheral neuropathy in the US. Diabetes Care 26: 1790-1795, 2003.
5. WEI ZX: Experiences in treating diabetic peripheral neuropathy with traditional Chinese medicine. Chin J Integr Med 14: 248-250, 2008.
6. Choi HJ, Kim NJ and Kim DH: Inhibitory effects of crude drugs on alpha-glucosidase. Arch Pharm Res 23: 261-266, 2000.

7. Chen F, Nakashima N, Kimura I and Kimura M: Hypoglycemic activity and mechanisms of extracts from mulberry leaves (folium mori) and cortex mori radicis in streptozotocin-induced diabetic mice. Yakugaku Zasshi 115: 476-482, 1995 (In Japanese).
8. Lian J, Chen J, Yuan Y, Chen J, Daud M Sayed M, Luo L, Zhu Y, Li S and Bu S: Cortex mori radicis extract attenuates myocardial damages in diabetic rats by regulating ERS. Biomed Pharmacother 90: 777-785, 2017.
9. Yin N, Hong X, Han Y, Duan Y, Zhang Y and Chen Z: Cortex mori radicis extract induces neurite outgrowth in PC12 cells activating ERK signaling pathway via inhibiting Ca(2+) influx. Int J Clin Exp Med 8: 5022-5032, 2015.
10. Hwang SH, Kang IJ and Lim SS: Antidiabetic effect of fresh nopal (opuntia ficus-indica) in low-dose streptozotocin-induced diabetic rats fed a high-fat diet. Evid Based Complement Alternat Med 2017: 4380721, 2017.
11. Lee MS, Park WS, Kim YH, Kwon SH, Jang YJ, Han D, Morita K and Her S: Antidepressant-like effects of Cortex Mori Radicis extract via bidirectional phosphorylation of glucocorticoid receptors in the hippocampus. Behav Brain Res 236: 56-61, 2013.
12. Yue HY, Yin C, Hou JL, Zeng X, Chen YX, Zhong W, Hu PF, Deng X, Tan YX, Zhang JP, *et al*: Hepatocyte nuclear factor 4alpha attenuates hepatic fibrosis in rats. Gut 59: 236-246, 2010.
13. Wesche-Soldato DE, Chung CS, Lomas-Neira J, Doughty LA, Gregory SH and Ayala A: In vivo delivery of caspase-8 or Fas siRNA improves the survival of septic mice. Blood 106: 2295-2301, 2005.
14. Taiana MM, Lombardi R, Porretta-Serapiglia C, Ciusani E, Oggioni N, Sassone J, Bianchi R and Lauria G: Neutralization of schwann cell-secreted VEGF is protective to in vitro and in vivo experimental diabetic neuropathy. PLoS One 9: e108403, 2014.
15. Gao F, Xiang HC, Li HP, Jia M, Pan XL, Pan HL and Li M: Electroacupuncture inhibits NLRP3 inflammasome activation through CB2 receptors in inflammatory pain. Brain Behav Immun 67: 91-100, 2018.
16. Gasperini R, Choi-Lundberg D, Thompson MJ, Mitchell CB and Foa L: Homer regulates calcium signaling in growth cone turning. Neural Dev 4: 29, 2009.
17. Livak KJ and Schmittgen TD: Analysis of relative gene expression data using real-time quantitative PCR and the 2(-Delta Delta C(T)) method. Methods 25: 402-408, 2001.
18. Coppey LJ, Shevalye H, Obrosov A, Davidson EP and Yorek MA: Determination of peripheral neuropathy in high-fat fed low-dose streptozotocin treated female C57Bl/6J mice and Sprague-Dawley rats. J Diabetes Investig 9: 1033-1040, 2018.
19. Schmidt RE, Parvin CA and Green KG: Synaptic ultrastructural alterations anticipate the development of neuroaxonal dystrophy in sympathetic ganglia of aged and diabetic mice. J Neuropathol Exp Neurol 67: 1166-1186, 2008.
20. Yang X, Yao W, Liu H, Gao Y, Liu R and Xu L: Tangluoning, a traditional Chinese medicine, attenuates in vivo and in vitro diabetic peripheral neuropathy through modulation of PERK/Nrf2 pathway. Sci Rep 7: 1014, 2017.
21. Kang TH, Moon E, Hong BN, Choi SZ, Son M, Park JH and Kim SY: Diosgenin from Dioscorea nipponica ameliorates diabetic neuropathy by inducing nerve growth factor. Biol Pharm Bull 34: 1493-1498, 2011.
22. Kim HJ, Lee HJ, Jeong SJ, Lee HJ, Kim SH and Park EJ: Cortex mori radicis extract exerts antiasthmatic effects via enhancement of CD4(+)CD25(+)Foxp3(+) regulatory T cells and inhibition of Th2 cytokines in a mouse asthma model. J Ethnopharmacol 138: 40-46, 2011.
23. You S and Kim GH: Protective effect of Mori Cortex radicis extract against high glucose-induced oxidative stress in PC12 cells. Biosci Biotechnol Biochem 83: 1893-1900, 2019.
24. Wang Y, Chen Z, Ye R, He Y, Li Y and Qiu X: Protective effect of jiaweibugan decoction against diabetic peripheral neuropathy. Neural Regen Res 8: 1113-1121, 2013.
25. Kim KJ, Namgung U and Cho CS: Protective effects of bogijetong decoction and its selected formula on neuropathic insults in streptozotocin-induced diabetic animals. Evid Based Complement Alternat Med 2017: 4296318, 2017.
26. Sarina, Yagi Y, Nakano O, Hashimoto T, Kimura K, Asakawa Y, Zhong M, Narimatsu S and Gohda E: Induction of neurite outgrowth in PC12 cells by artemisinin through activation of ERK and p38 MAPK signaling pathways. Brain Res 1490: 61-71, 2013.
27. Zhang D, Chan JD, Nogi T and Marchant JS: Opposing roles of voltage-gated Ca2+ channels in neuronal control of regenerative patterning. J Neurosci 31: 15983-15995, 2011.
28. Balasubramanyam M, Balaji RA, Subashini B and Mohan V: Evidence for mechanistic alterations of Ca2+ homeostasis in type 2 diabetes mellitus. Int J Exp Diabetes Res 1: 275-287, 2001.
29. Verkhratsky A and Fernyhough P: Mitochondrial malfunction and Ca2+ dyshomeostasis drive neuronal pathology in diabetes. Cell Calcium 44: 112-122, 2008.
30. Cao XH, Byun HS, Chen SR and Pan HL: Diabetic neuropathy enhances voltage-activated Ca2+ channel activity and its control by M4 muscarinic receptors in primary sensory neurons. J Neurochem 119: 594-603, 2011.
31. Chandramoorthy HC, Bin-Jaliah I, Karari H, Rajagopalan P, Ahmed Shariff ME, Al-Hakami A, Al-Humayad SM, Baptain FA, Ahmed HS, Yassin HZ and Haidara MA: MSCs ameliorates DPN induced cellular pathology via [Ca2+]i homeostasis and scavenging the pro-inflammatory cytokines. J Cell Physiol 233: 1330-1341, 2018.
32. Louhivuori LM: Calcium a key player in early neural development and migration: TRPCs and VGCCs. Argumentation 1: 201-207, 2015.
33. Li M, Chen C, Zhou Z, Xu S and Yu Z: A TRPC1-mediated increase in store-operated Ca2+ entry is required for the proliferation of adult hippocampal neural progenitor cells. Cell Calcium 51: 486-496, 2012.
34. Kruglikov I, Gryshchenko O, Shutov L, Kostyuk E, Kostyuk P and Voitenko N: Diabetes-induced abnormalities in ER calcium mobilization in primary and secondary nociceptive neurons. Pflugers Arch 448: 395-401, 2004.
35. Song E, Lee SK, Wang J, Ince N, Ouyang N, Min J, Chen J, Shankar P and Lieberman J: RNA interference targeting Fas protects mice from fulminant hepatitis. Nat Med 9: 347-351, 2003.
36. Vigont V, Kolobkova Y, Skopin A, Zimina O, Zenin V, Glushankova L and Kaznacheyeva E: Both Orai1 and TRPC1 are involved in excessive store-operated calcium entry in striatal neurons expressing mutant huntingtin Exon 1. Front Physiol 6: 337, 2015.
37. Chen HC, Wang CH, Shih CP, Chueh SH, Liu SF, Chen HK and Lin YC: TRPC1 is required for survival and proliferation of cochlear spiral ganglion stem/progenitor cells. Int J Pediatr Otorhinolaryngol 79: 2290-2294, 2015.
38. Shim S, Yuan JP, Kim JY, Zeng W, Huang G, Milshteyn A, Kern D, Muallem S, Ming GL and Worley PF: Peptidyl-prolyl isomerase FKBP52 controls chemotropic guidance of neuronal growth cones via regulation of TRPC1 channel opening. Neuron 64: 471-483, 2009.
39. Heo DK, Chung WY, Park HW, Yuan JP, Min GL and Kim JY: Opposite regulatory effects of TRPC1 and TRPC5 on neurite outgrowth in PC12 cells. Cell Signal 24: 899-906, 2012.
40. Zhang D, Freedman BI, Flekac M, Santos E, Hicks PJ, Bowden DW, Efendic S, Brismar K and Gu HF: Evaluation of genetic association and expression reduction of TRPC1 in the development of diabetic nephropathy. Am J Nephrol 29: 244-251, 2009.
41. Krout D, Schaar A, Sun Y, Sukumaran P, Roemmich JN, Singh BB and Claycombe-Larson KJ: The TRPC1 Ca^{2+}-permeable channel inhibits exercise-induced protection against high-fat diet-induced obesity and type II diabetes. J Biol Chem 292: 20799-20807, 2017.
42. Yu JS and Cui W: Proliferation, survival and metabolism: The role of PI3K/AKT/mTOR signalling in pluripotency and cell fate determination. Development 17: 3050-3060, 2016.
43. Li R, Li Y, Wu Y, Zhao Y, Chen H, Yuan Y, Xu K, Zhang H, Lu Y, Wang J, *et al*: Heparin-poloxamer thermosensitive hydrogel loaded with bFGF and NGF enhances peripheral nerve regeneration in diabetic rats. Biomaterials 168: 24-37, 2018.
44. Chen L, Gong HY and Xu L: PVT1 protects diabetic peripheral neuropathy via PI3K/AKT pathway. Eur Rev Med Pharmacol Sci 22: 6905-6911, 2018.
45. Zhang YP, Liu SY, Sun QY, Ren J, Liu HX and Li H: Proanthocyanidin B2 attenuates high-glucose-induced neurotoxicity of dorsal root ganglion neurons through the PI3K/Akt signaling pathway. Neural Regen Res 13: 1628-1636, 2018.